

Nano-scale Flexible Interphase in a Glass Fiber/Epoxy Resin System Obtained by Admicellar Polymerization

Harry J. Barraza^(a), Levent Aktas^(b), Youssef Hamidi^(b), Edgar A. O'Rear^(a), and M.C. Altan^(b)
^(a) School of Chemical Engineering and Materials Science, University of Oklahoma, Norman, OK 73019
^(b) School of Aerospace and Mechanical Engineering, University of Oklahoma, Norman, OK 73019

Abstract

Organosilane coupling agents are widely used in the composites industry to improve the wetting of inorganic reinforcements by low surface energy resins. An increased wettability is often a harbinger of better mechanical properties in a structural composite. Silane coatings effectively increase the spreading of liquid matrixes over glass reinforcement by altering the surface energetics of glass, not by extensive coverage, but by eradication of the high-energy sites present in the oxide surface. Commercial sizings often applied to glass fibers contain up to 10% of the active silane agent, while the remaining 90% is a mixture of lubricants, surfactants, anti-stats, and film formers. Recent investigations have demonstrated that non-reactive components tend to remain in high concentrations within the interphase, thus weakening the resin network crosslink density and increasing the potential for water ingress. Further, sizing formulations are proprietary and designed for specific resin system, which make them expensive, consequently limiting their widespread use.

In this paper, admicellar polymerization, a versatile technique to prepare elastomeric thin films of styrene-isoprene copolymer and polystyrene on the surface of random glass-fiber mats is presented. This hydrophobic coating of monolayer thickness applied to the glass fibers is not expected to disrupt the matrix cross-linking reaction; and due to its higher elastic modulus, is believed to cause a change in the stress distribution along the fiber length. Admicellar-modified reinforcements were impregnated with an epoxy resin system: EPON 815C/EPICURE 3232, and molded by Resin Transfer Molding (RTM) into disk shaped parts. Tensile strength, stiffness and interlaminar shear strength (ILSS) were measured for the flexible interphase composites, and compared to parts containing commercially sized and bare fibers. Void fraction, void size and shape distributions, as well as water diffusivity were investigated for each system.

Introduction

The structural integrity and lifetime performance of fiber-reinforced composites are highly dependent upon the stability of the interfacial region located between the matrix and fiber surfaces. For glass fibers, modification of the surface by means of organosilane coupling agents is the standard commercial approach because these agents have proven to be an effective way to enhance the adhesion of glass fibers to many thermoset polymer matrixes, including epoxies. However, these proprietary formulations are often expensive and designed for specific resin systems. The thicknesses of the sizings that have dominated the glass-reinforcement market lie in the range between 0.1 μm and 0.5 μm , and are commonly applied as a solvent mixture containing only a small percentage of active coupling agent (ca. 10%)¹. Deficiencies in the composites performance related to excessive non-reactive components (e.g. binding agent) have led researchers to focus their attention to creating monomolecular, reactive surface layers which may strongly interact with both the organic and inorganic constituents present at the interphase². DiBenedetto³ points out that monolayer and submonolayer coatings can improve interfacial bond strength when one end of the molecule is tethered to the surface of the reinforcement and the functional groups or polymeric chains on the other end react and/or interpenetrate the matrix phase. Examples of such an approach include the attachment of tethered polysulfone⁴, as well as polystyrene⁵ chains to the surface of E-glass fibers. In the case of polystyrene, it was confirmed that a low attachment density was required to provide optimum mixing with the matrix free chains and, thus, higher interfacial bonding strength. Our research group has recently introduced an alternative surface modification method applicable to glass fibers that uses surfactants and elastomeric monomers. Admicellar polymerization is the term used to

describe this procedure and involves the formation of a polymeric film on the fiber surface with a thickness well below 100 nm. Characterization studies of these thin polymeric coatings through contact angle measurements⁶ confirmed the hydrophobic nature of the modified surface, and suggested the establishment of an adequate level of surface energy interactions between admicellar-modified glass fibers and a DGEBA-type epoxy resin (e.g. EPON 815C). The current work is dedicated to investigate the effect of sizing type, architecture and void content to strength, stiffness, interlaminar shear strength (ILSS) and moisture absorption rate of disk-shaped parts molded by RTM.

Experimental studies

FibreGlast boron-free E-glass fibers (Plast # 248) were used in all cases as the inorganic reinforcement phase for the fabricated composite parts. These fibers were subjected to different pretreatments and posttreatments depending on the type of sizing to be applied: (a) Heat cleaned at 500 °C for 15 minutes, as in the case of the control samples; (b) Heat cleaned and then equilibrated with a 7000 µM surfactant solution (SDS), pure styrene or styrene/isoprene monomer mixture. Monomers partition into the surface aggregates created by the surfactant moieties, and with the aid of an oil-soluble azo-initiator (AIBN) in mild temperatures (80 to 90 °C) polymerize into an admicellar-coated polystyrene or styrene-isoprene glass surface. Further details concerning the admicellar-coating technique can be found elsewhere⁶. The admicellar treatment unavoidably caused a complete disruption of the original planar random-mat architecture that both the commercial silane-coated fibers and control fibers had. Hence, the experiments aimed to test the different sizings were performed with fibers that were manually pulled apart from the original mat and meticulously positioned inside a 58-cm³ disk-shaped aluminum mold (Figure 1), maintaining a randomly distributed fiber orientations with a non-layered structure. 30 g of fibers were set inside the mold cavity, which represents a fiber volume fraction of approximately 21 % in all composite parts fabricated. For comparison purposes, parts containing the same volume fraction but with a random two-dimensional layered architecture of silane coated and desized fibers were also molded at the same resin infiltration velocity. The complete set of experiments and conditions are summarized in Table 1.

A molding press was designed and built in such way that the two-component epoxy resin system (EPON 815C and EPICURE 3282) would be injected at a constant rate around 5.32 cm³/s. Figure 2 depicts the basic components of the filling fixture. The moving plate and the plungers were secured to the ram of a 40-ton hydraulic press (ARCAN, Model CP402). The stainless-steel cylinders were welded to a steel plate placed perpendicular to the plungers, which was held in place on the press body with c-clamps. The internal diameters of the two cylinders containing the resin and curing agent were: 55.47 mm and 25.53 mm in order to achieve the appropriate mix ratio, 4.7 to 1 by volume, of resin to curing agent. The flow coming from both cylinders was thoroughly mixed by passing it through an 18.6 cm-long polypropylene in-line Statomix® mixer (Technical Resin Packaging Inc), and subsequently injected into the sealed, center-gated molds, that vented air by four ports located 90° apart during filling. After filling, the four vents were closed to allow the application of an extra post-fill packing pressure on the molds, which has been found to be beneficial for the mechanical performance of liquid-molded parts⁷. As the final step, the inlet hose is clamped to maintain the pressure, and the part left for 24 hours inside the mold until it reached the so-called “green” state when it could be taken out of the mold without difficulty. Typically, two molds containing the same type of fibers were impregnated concurrently by dividing the outflow from the mixer with a plastic tee. The average fill time for both molds was 20 seconds. With the resin and curing agent contained in the cylinders it was possible to impregnate three pairs of disks of different sizing types. A total of 10 to 12 disks for each sizing type were fabricated under the same conditions.

Each molded disk was sectioned using a vertical milling machine into five rectangular specimens with dimensions: 11.43 cm x 1.27 cm x 0.4 cm; and thereafter polished on the sides with a 320 grit sand paper to even out the asperities left by the cutting bit. The relative spatial positions of the five

specimens within each molded disk is presented in Figure 3. Specimens marked 1 and 2 from all molded disks were tested under tension according to ASTM D3039/D3039M-00 standard. Tensile forces applied were ramped linearly from 0 to 8.90 kN over 120 seconds. Strain measurements were obtained simultaneously with the tensile strength tests by placing a calibrated extensometer over a 2.54 cm span at the center of the specimen. Specimen 3, which is located at the center of the disk, did not comply with the requirements for mechanical testing because of the presence of surface defects at the inlet gate caused during the demolding process. As such, these center specimens were used later for void content and morphometry analysis. Specimen 4 demanded further sectioning to fit into the special three-point bend fixture (MTS 642.001) that was used to measure the interlaminar shear strength (ILSS). With the aid of a band saw, three identical, 3.8 cm-long coupons were cut out from specimen 4, and only the coupon located in the central position was used for testing. The MTS 810 machine moving at a crosshead speed of 1.0 mm/min provided the force applied to the specimen during the three-point bend test, and the experimental parameters such as the maximum force and maximum displacement were measured and recorded automatically by the system. Interlaminar strength and other relevant calculations were performed in accordance with the ASTM D2344/D2344M-00 standard. Finally, specimen 5 was utilized to investigate the hygrothermal resistance of admicellar-coated interfaces by immersing the samples in a temperature-controlled water bath at 45 °C and periodically registering the weight gain according to the procedures described by the ASTM D 5229M standard. Prior to the water immersion, the specimens were dried in a vacuum oven for seven days at 65 °C under a vacuum of 25 in Hg.

Results

Within the admicellar polymerization treatment, heat-cleaned glass fibers were contacted with a surfactant solution containing the reacting monomers under moderate mixing conditions. As mentioned before, such treatment caused a complete disruption of the original planar random-mat architecture the desized fibers initially had. This wider pore space in the nonlayered reinforcement brought about a more favorable resin impregnation, which in part explains the negligible void content values listed for these samples on Table 1. Given that the intrabundle space was almost inexistent, the voids were all located in resin-rich areas, with a higher occurrence of small diameter (ca. 60 μm) bubbles of circular to ellipsoidal shape as the one depicted in Figure 4a. Isolated voids of bigger diameter, as the one depicted in Figure 4b, were very infrequent and all had circular shapes. Another effect arising from the introduction of reinforcements with higher interfiber distance is a manifest reduction in all the mechanical parameters measured, as compared to the properties of random-layered composites. An average decrease of 15.2% in the ultimate tensile strength, as well as a 6% decrease in stiffness and 9.8% in the interlaminar shear strength, took place within the sized samples (I → Im). For the desized composites (II → IIm), the average UTS and stiffness is reduced by similar percentages: 11% and 10.5% respectively. No statistical difference was found for the interlaminar shear strength of desized samples (II vs. IIm); although the test did show a noticeable decrease (ca. 11.4%) in the interlaminar adhesion attributed to the desizing process (IIm vs. Im). Data for both architectures and sizing types are presented in Figures 5a-5c and Figures 6a-6c. These results are suggestive of more catastrophic failure mechanisms acting on composites with nonlayered structure. Seemingly, crack-tip blunting or crack arrest can be performed more effectively by a layered bundle of fibers⁸.

Regardless of the fiber architecture, the experiments showed a marked influence of the commercial sizing on the final mechanical properties of the composites parts. Silane-coated fibers always performed significantly better than the composites fabricated with control fibers in both tensile and flexural tests. In the specific case of nonlayered reinforcement with commercial sizing (Im), the results show appreciably high increases in UTS and stiffness values, 23% and 29% respectively, when compared to the control samples (IIm). Only a moderate increase (ca. 13%) resulted in the interlaminar shear strength for the same type of sizing. In the case of the flexible interphase formed by admicellar polymerized styrene-isoprene (IV), the ultimate tensile strength turned out to be 11.7%

higher than the desized control sample, whereas the stiffness showed an increase up to 13.7%. A statistical analysis using the t-test revealed that although significantly high data variability may exist, particularly in the tensile mode (Coefficient of Variation, CV = 17%), there is suggestive evidence ($p < 0.075$) that the elastomeric-coated fibers behave differently from the control samples in the aforementioned tests. The statistical difference supporting the better performance of samples IV against the control sample (II_m) is even stronger after analyzing the results for the three-point bend tests ($p < 0.002$). From Figure 6c it appears that simply by introducing a thin film of elastomeric nature the interlaminar shear strength of the composite may be improved by almost 31% as compared to a completely bare fiber. In contrast to the styrene-isoprene copolymer, no previous evidence about polystyrene sizing compatibility with the epoxy resin was available. However, single-fiber contact angle experiments with water yielded advancing angles that were close to 70 degrees, which unequivocally demonstrates the hydrophobic character of the polystyrene-coated reinforcement. Average values for the three mechanical parameters measured on composites fabricated with polystyrene-coated reinforcement are also presented in Figure 6a to 6c. The ultimate tensile strength for the composites type III reached a value 15.5% higher, in average, than the one attained by the control sample. Considerably lower increases in stiffness, 8.1%, and interlaminar adhesion, 5.6%, were observed for this kind of sizing with respect to the desized composites. Although it would be tempting to conclude that these results support the expectation of a positive influence from the polystyrene coating, the coefficient of variation for this particular data set was so high that, in general, the values reported as the “average” for each specific property are not very representative of the sample dispersion. CV's in the order of 25% to 35% were detected, and this in fact obscures any slight differences in mechanical behavior between composites type III and the control samples (II_m). P-values found during the statistical analysis were: 0.105 for the UTS; 0.300 for the stiffness; and 0.334 for the interlaminar shear strength. Based on these statistical probabilities, the t-test showed little or no real evidence to conclude that a difference in mechanical performance operates as a result of introducing the polystyrene thin film as a sizing.

Extending the observations reported previously in the literature to our admicellar system, it appears that the differences in sizing performance for composites type III and type IV may be related to a higher segmental motion, and consequently more effective interdiffusion occurring between the styrene-isoprene chains and the long epoxy segments present in the matrix before gelation. Admittedly, other factors like chain structure (e.g. linear for polystyrene, and branched for styrene-isoprene), as well as the presence of unsaturated moieties in the isoprene block branches, may also contribute to augment the interactions between styrene-isoprene and the epoxy functional groups. However, at this point it is believed that a combined effect of reduced sizing thickness and glass transition temperatures well below the room temperature is responsible for the noticeably increased flexural properties of type IV composites. Recent examples in the literature confirm our hypothesis that a thin elastomeric sizing of significantly low T_g would originate positive changes in the mechanical performance of composite materials. For instance, Tillie⁹ showed that it is possible to promote better impact strength properties of unidirectional composites, without any detriment to the stiffness, by introducing a hybrid elastomeric interphase composed of hydroxylated polydimethylsiloxane (PDMS) with a glass transition temperature of -115 °C. Commercial sizings often include in their formulations elastomeric agents that are miscible but non-reactive with the polymeric matrix¹. These elastomers have T_g values in the same order of magnitude than the glass transition temperature of the styrene-isoprene thin films used herein. However, once the elastomer is mixed with organosilanes and other additives (e.g. surfactants) it is very likely that the glass transition temperature of the composite film acting as the sizing would rise to much higher values than that for the original rubber. Although the sizing present in composites type I and Im were only known to be epoxy-compatible, no details about the exact composition or the introduction of rubbery agents were available to us. A higher glass transition temperature and a thicker film, resulting from a greater number of components, may explain in part the poorer flexural properties observed for composites fabricated with commercial sizings (Figure 6c) as opposed to those composites with reinforcements sized with a polymeric film only several nanometers thick. These results have implications for

composite manufacture applications because they show the possibility of creating tailored interfaces from pure polymers with relatively low market prices.

The combination of highly hygroscopic materials such as glass fibers and oxygen-containing polymers (e.g. epoxies) make glass-fibers/epoxy composites especially susceptible to water ingress. It is well known that water accumulates at unprotected glass fibers over a period of time causing both loss of adhesion and a reduction of fiber strength³. Therefore, by covering the hydrophilic glass surface with polymers with good water-repellency properties it is expected to prevent the water accumulation phenomenon and consequently the adhesive bond rupture. Figures 7a to 7h show the moisture absorption rate and moisture saturation values for all sizing types investigated. Focusing on the average maximum moisture content, it is evident that amine cross-linked epoxy polymers such as the EPON/EPICURE system used in this study have the ability of absorbing high amounts of water at the temperature conditions set for the hygrothermal experiments (45 °C). The neat resin sample (N) accumulated a maximum of nearly 2.6% w/w of water, which was the largest increase registered for all samples studied. From Dynamic Mechanical Analysis (DMA) tests it was observed that physical and/or chemical interaction of the glass-fiber surface with the epoxy matrix reduces the chain mobility, leading to a rise in the glass transition temperature (T_g) from around 60 °C to 75 °C. Thus, given the lower T_g of the neat resin it is reasonable to anticipate an increased free volume in the chain packing of the polymer at the temperature conditions set for the hygrothermal experiments, facilitating faster water absorption rates. The desized fiber composites with layered (II) and nonlayered (II_m) fibers had average moisture saturation values slightly lower than the neat resin, but substantially higher than any other sized composite either commercial or admicellar-treated. These results are in accordance to what has been observed previously in the literature and shows that the driving force for water absorption is very much dependent on the hydrophilic characteristics of the glass fibers. In those composites with coated reinforcements (I, Im, III and IV) the moisture saturation values were greatly reduced. It is worth noting that independent of fiber architecture (i.e. layered or nonlayered) the percent moisture content at equilibrium was always smaller than 2%. Intriguingly, samples III and IV that had a more hydrophobic sizing showed maximum water absorption values 10% smaller than the commercial samples; although in the case of specimens III the data scatter was more pronounced than sample IV. This may constitute a possible indication of a reduction in the capillarity transport of water through the intrabundle space due to a modified glass surface exhibiting higher contact angles with respect to water.

In addition to moisture saturation levels, the other parameter reflecting in part the final performance of composites under wet conditions is the diffusion rate behavior. The diffusion rate constant (D_z) for the specimens was calculated according to equation 1, as specified by ASTM 5259:

$$D_z = \pi \left(\frac{h}{4M_m} \right)^2 \left(\frac{M_2 - M_1}{\sqrt{t_2} - \sqrt{t_1}} \right)^2 \quad (1)$$

where h is the specimen thickness, M_m is the moisture saturation level, and the quantity in the second parenthesis is the slope of the initial region on a plot of moisture weight gain vs. the square root of time. As observed in Figures 7a to 7g all the composite specimens followed the Fickian diffusion approximation and exhibited initial linear regions that in all cases extended to moisture levels close to the 60% of the saturation value. Calculated values for D_z are plotted with 95% confidence intervals in Figure 7h. The diffusion rate behavior of the control samples reaffirms the preliminary conclusions drawn from the maximum saturation levels in showing the importance of sizings in the reduction of water ingress levels. There is a remarkable difference in the water diffusion rates for layered composites with and without commercial sizing, which may be intensified by the higher capillary pressures generated in a more compact intrabundle space. With a wider pore space (nonlayered structure), the sizing effect on the diffusion constant is present but it is not as strong as in the layered

structure case. Further evidence of the close relationship between capillary pressure and diffusion rate is found by contrasting diffusion coefficients for the neat resin (N) and the layered desized-composite (II), shown in Figure 7h. At equilibrium, the neat resin reaches an expected higher saturation value due to its lower T_g . However, the rate at which the water penetrates the composite (D_z) is faster for the composite sample than the neat resin despite its much higher T_g . Diffusion coefficients for samples Im, III and IV were statistically identical, which may be interpreted as a positive sign of the resistance of composites with a nano-scale sizing to long-term exposure to humid environments.

Conclusions

In this paper the possibility of utilizing the admicellar polymerization technique to create a nano-scale elastomeric sizing over glass fiber reinforcements is demonstrated. Resin transfer molded parts fabricated with random, nonlayered glass-fiber preforms coated with a very thin styrene-isoprene sizing showed a moderate increase in strength and stiffness with respect to the control samples. In addition, flexural properties measured by the three-point bend test were improved in more than 30% from the control level and statistically comparable to the interlaminar shear strength level attained by the proprietary commercial sizings. It appears that positive effects coming from the introduction of a nanometer-thick elastomeric interlayer can be noticed only if extensive cooperative segmental motions are present, that is, when the glass transition temperature of the admicellar-polymerized thin films is far below the room temperature. This fact was particularly seen in the case of polystyrene thin films used as sizing in composites type III, where no beneficial effects could be detected. Moisture saturation and diffusion rate constants measured in hygrothermal experiments performed at 45 °C showed admicellar-treated fibers can achieve slightly higher water-repellency levels than those of silane-coated reinforcements. Work in progress will attempt to perfect the admicellar-film coverage to create more available sites for chemical/physical interaction, as well as to extend the use of this polymerization technique to obtain new sizings from elastomers with a much lower glass transition temperature than the styrene-isoprene.

References

1. J.L. Thomason and L.J. Adzima, *Sizing up the interphase: an insider's guide to the science of sizing*, Composites: Part A, **32**, pp. 313-321 (2001)
2. H. Ishida and T. Chaisuwan, *Tailoring the interphase of glass fiber-reinforced benzoxazine composites: Effect of fiber surface treatment*, Proc. Amer. Chem. Soc., PMSE Div., **85**, pp. 534-535 (2001)
3. A.T. DiBenedetto, *Tailoring of interfaces in glass fiber reinforced polymer composites: a review*, Mater. Sci. Eng., **A302**, pp. 74-82 (2001)
4. A.T. DiBenedetto, S.J. Huang, D. Birch, J. Gomez and W.C. Lee, *Reactive coupling of fibers to engineering thermoplastics*, Composite Structures, **27**, pp. 73-82 (1994)
5. R. Lin, R.P. Quirk, J. Kuang and L.S. Penn, *Toughening of impenetrable interfaces by monodisperse tethered polymer chains: effect of areal attachment density*, J. Adhesion Sci. Technol., **10**, pp. 341-349 (1996)
6. H.J. Barraza, M.J. Hwa, K. Blakely, E.A. O'Rear and B.P. Grady, *Wetting behavior of elastomer-modified glass fibers*, Langmuir, **17**, pp. 5288-5296 (2001)
7. K.A. Olivero, H.J. Barraza, E. A. O'Rear and M.C. Altan, *Effect of injection rate and post-fill cure pressure on properties of resin transfer molded disks*, J. Compos. Mater., in press (2002)
8. J. Varna, R. Joffe, L.A. Berglund and T.S. Lundström, *Effect of voids on failure mechanisms in RTM laminates*, Compos. Sci. Technol., **53**, pp. 241-249 (1995)
9. M.N. Tillie, T.M. Lam, J.F. Gérard, J.F., *Insertion of an interphase synthesised from a functionalised silicone into glass-fibre/epoxy composites*, Compos. Sci. Technol., **58**, 659-663 (1998)

Table 1 - Experimental conditions and void content

| Sample Code | Sizing Type | Fiber surface pretreatment/posttreatment | Preform architecture | Void Content (%) |
|--------------------|-----------------------------|---|-------------------------------|-------------------------|
| N | None | None | Neat resin | 0 |
| I | Commercial epoxy-compatible | None | Random mats. 4 layers stacked | 0.18 ± 0.2 |
| II | None | 500 °C for 15 min. | Random mats. 4 layers stacked | 0.006 ± 0.002 |
| Im | Commercial epoxy-compatible | None | Fiber tows pulled-apart | <0.005 |
| IIm | None | 500 °C for 15 min. | Fiber tows pulled-apart | <0.005 |
| III | Polystyrene | 500 °C for 15 min + admicellar polymerization | Fiber tows pulled-apart | <0.005 |
| IV | Styrene-isoprene copolymer | 500 °C for 15 min + admicellar polymerization | Fiber tows pulled-apart | <0.005 |

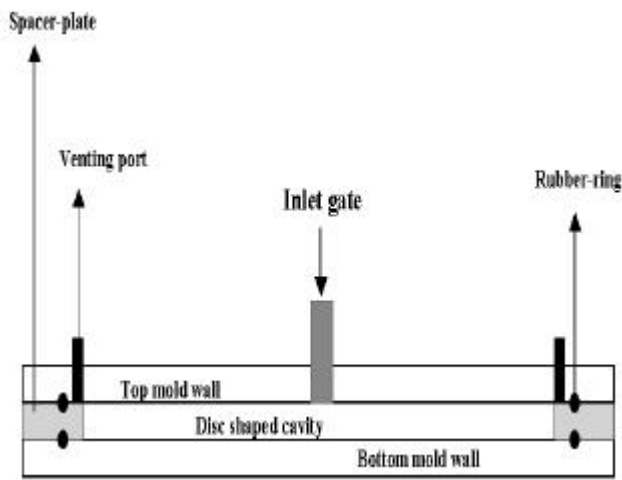


Figure 1 - Aluminum mold cross-section

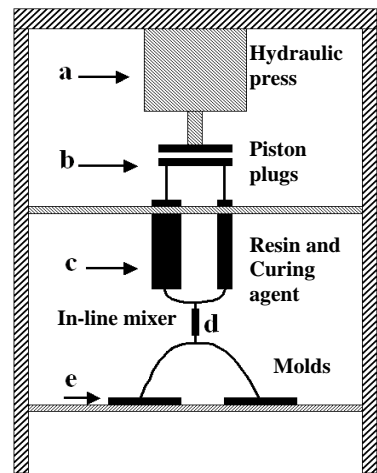


Figure 2 - RTM filling fixture

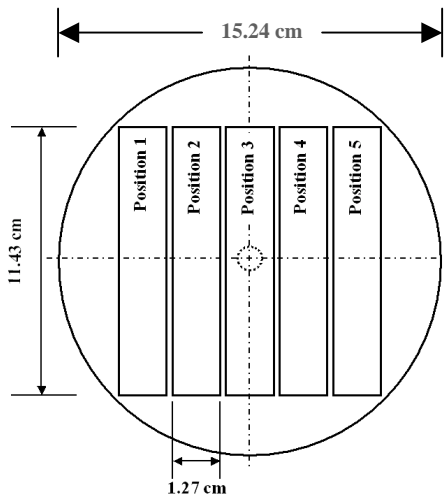


Figure 3 - Test specimens in a molded disk

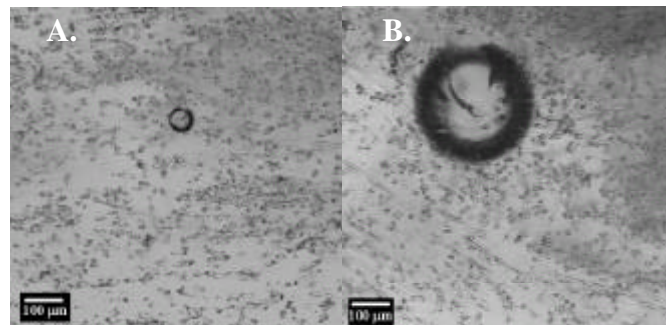


Figure 4 - Voids in nonlayered composites

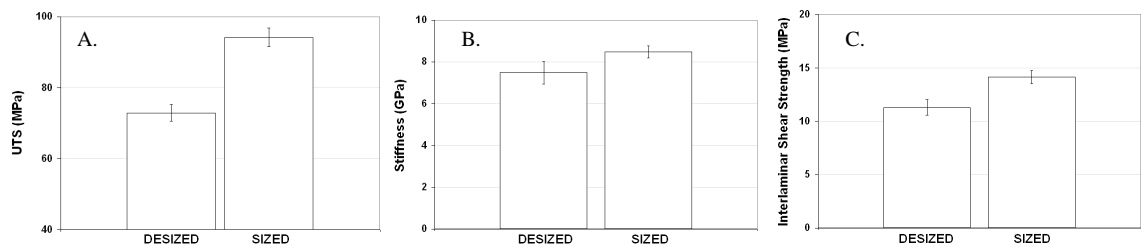


Figure 5 - Mechanical properties of composites with layered structure

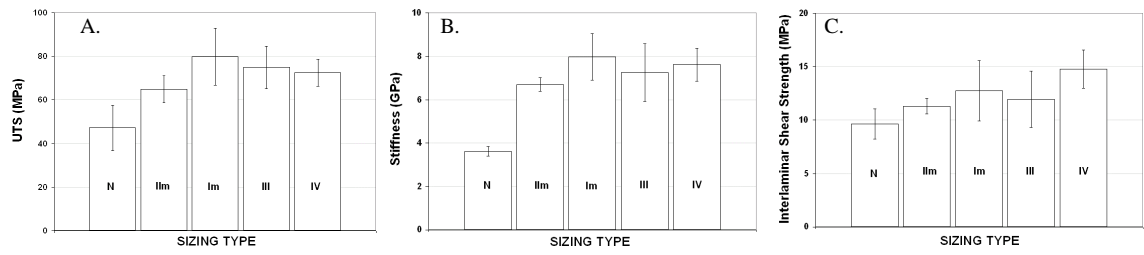
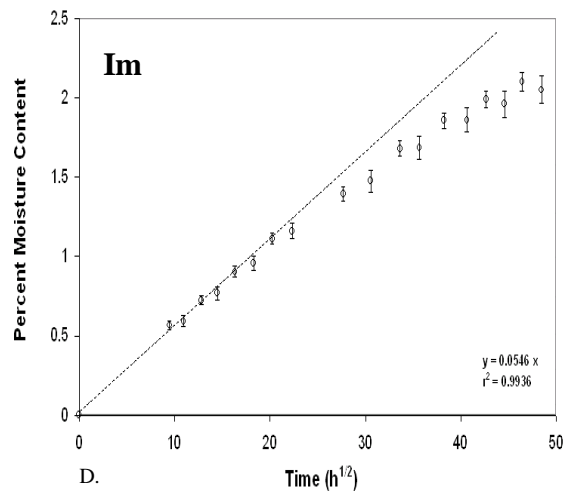
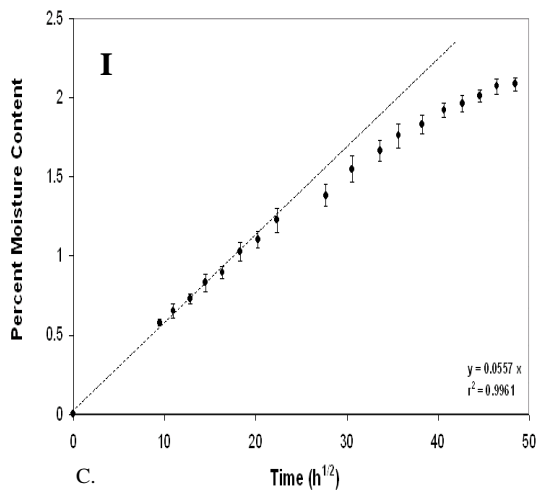
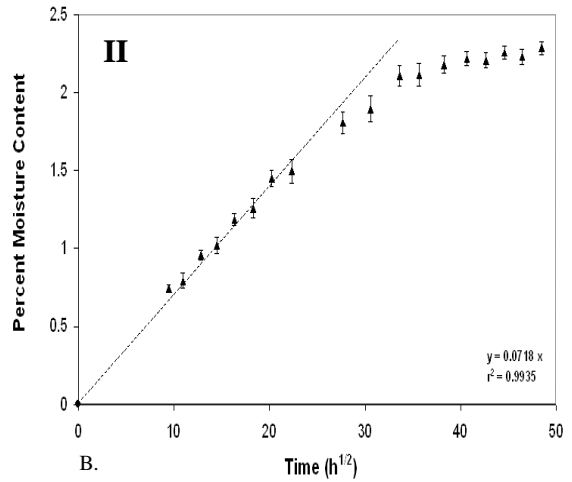
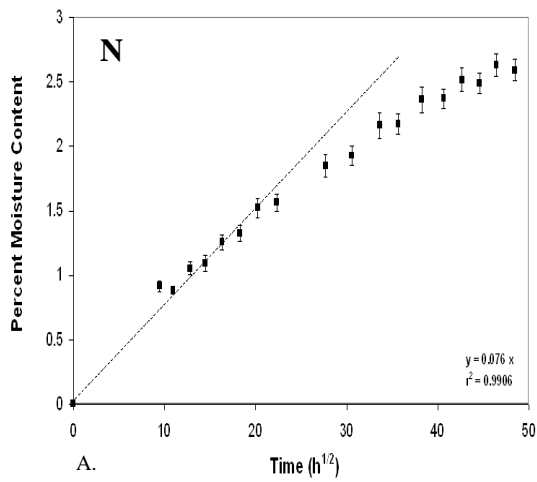


Figure 6 - Mechanical properties of composites with nonlayered structure



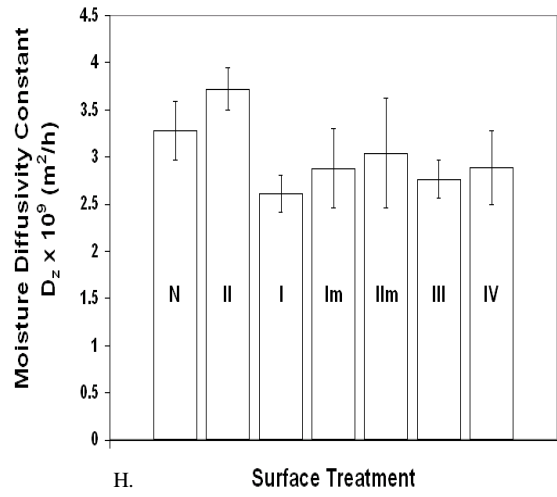
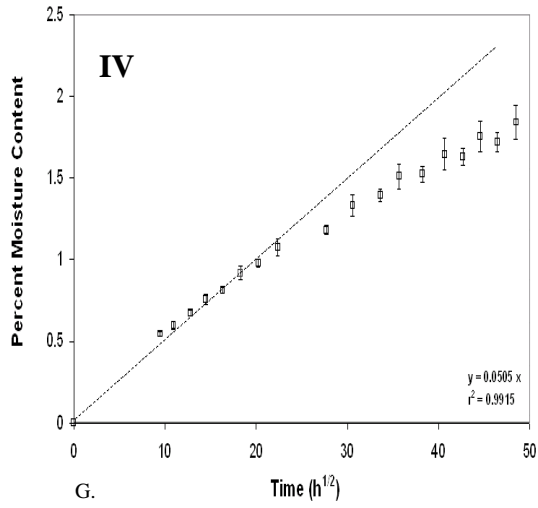
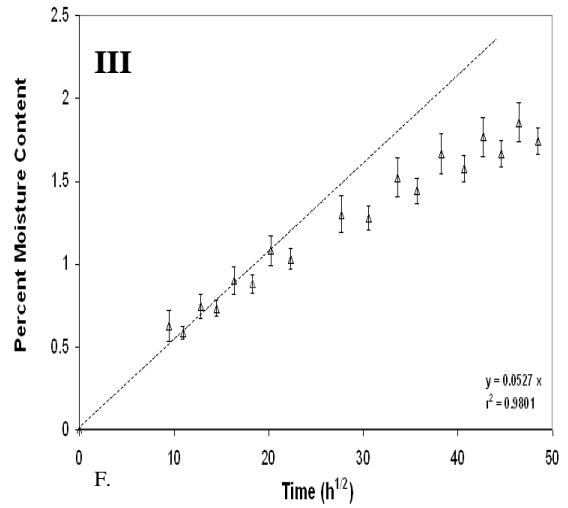
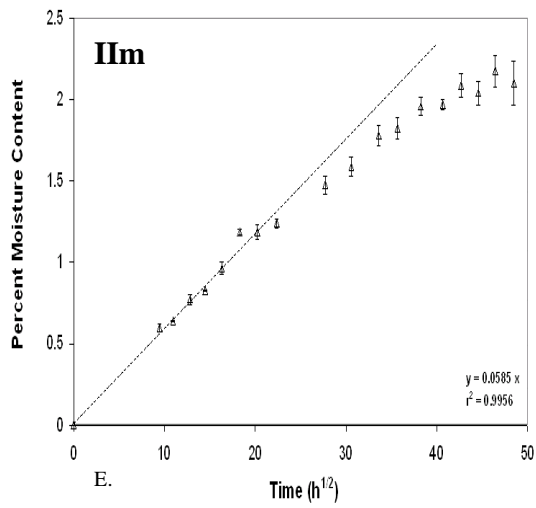


Figure 7 - Moisture saturation levels and diffusion coefficients for RTM molded composites